THE EUROPEAN
PHYSICAL JOURNAL C

Lorentz invariance violation in the neutrino sector: a joint analysis from big bang nucleosynthesis and the cosmic microwave background

Wei-Ming Dai[1,3,a], **Zong-Kuan Guo**[1,2,b], **Rong-Gen Cai**[1,3,c], **Yuan-Zhong Zhang**[1,d]

[1] CAS Key Laboratory of Theoretical Physics, Institute of Theoretical Physics, Chinese Academy of Sciences, P.O. Box 2735, Beijing 100190, China
[2] School of Astronomy and Space Science, University of Chinese Academy of Sciences, No. 19A Yuquan Road, Beijing 100049, China
[3] School of Physical Sciences, University of Chinese Academy of Sciences, No. 19A Yuquan Road, Beijing 100049, China

Abstract We investigate constraints on Lorentz invariance violation in the neutrino sector from a joint analysis of big bang nucleosynthesis and the cosmic microwave background. The effect of Lorentz invariance violation during the epoch of big bang nucleosynthesis changes the predicted helium-4 abundance, which influences the power spectrum of the cosmic microwave background at the recombination epoch. In combination with the latest measurement of the primordial helium-4 abundance, the Planck 2015 data of the cosmic microwave background anisotropies give a strong constraint on the deformation parameter since adding the primordial helium measurement breaks the degeneracy between the deformation parameter and the physical dark matter density.

1 Introduction

Neutrino oscillations have shown that there are small but nonzero mass squared differences between three neutrino mass eigenstates (see Ref. [1] and the references therein), which imply the existence of physics beyond the standard model of particle physics. However, neutrino oscillation experiments cannot tell us the overall mass scale of neutrinos. Fortunately, cosmology provides a promising way to determine or constrain the total mass of neutrinos by the gravitational effects of massive neutrinos which can significantly change the CMB power spectrum due to lensing [2–5] and the formation of large-scale structures [6,7], therefore, alter

the cosmic microwave background (CMB) anisotropies and the large-scale structure distribution of matter (see [8] for a review). Recent Planck 2015 data combined with some low-redshift data give an upper limit on the total mass of neutrinos at 95% confidence level, $\Sigma m_\nu < 0.19$ eV [5].

Another possible signal of new physics is Lorentz invariance violation in the neutrino sector. The observed neutrino oscillations may originate from a combination of effects involving neutrino masses and Lorentz invariance violation [9–14]. Lorentz invariance is a fundamental symmetry in the standard model of particle physics. Although present experiments have confirmed Lorentz invariance to a good precision [15], it may be broken in the early Universe when energies approach the Planck scale. The standard model itself is believed to be a low-energy effective theory of an underlying unified theory. Lorentz invariance violation has been explored in quantum gravity [16], loop quantum gravity [17], non-commutative field theory [18], and doubly special relativity theory [19]. Various searches for Lorentz invariance violation have been performed with a wide range of systems [20,21].

The cosmological consequences of neutrinos with the Coleman–Glashow type [10] dispersion relation have been studied in Ref. [22]. As can be expected, the Lorentz-violating term affects not only the evolution of the cosmological background but also the behavior of the neutrino perturbations. The former changes the expansion rate prior to and during the epoch of photon–baryon decoupling, which alters heights of the first and second peaks of the CMB temperature power spectrum, while the latter alters the shape of the CMB power spectrum by changing neutrino propagation. Since these two effects can be distinguished from a change in the total mass of neutrinos or in the effective number of

[a] e-mail: daiwming@itp.ac.cn

[b] e-mail: guozk@itp.ac.cn

[c] e-mail: cairg@itp.ac.cn

[d] e-mail: zyz@itp.ac.cn

extra relativistic species, CMB data have been proposed as a probe of Lorentz invariance violation in the neutrino sector.

Moreover, since the Lorentz-violating term influences the abundances of the light elements by altering the energy density of the Universe and weak reaction rates prior to and during the Big bang nucleosynthesis (BBN) epoch, BBN provides a promising probe of Lorentz invariance violation in the neutrino sector in the early Universe [23]. In particular the BBN-predicted abundance of helium-4 is very sensitive to the Lorentz-violating term. It is well known that the primordial helium-4 abundance plays a non-negligible role at the recombination epoch because it has an influence on the number density of free electron. Therefore, Lorentz invariance violation affects the CMB power spectrum by changing the BBN-predicted abundance of helium-4. A reasonable way to test Lorentz invariance violation in the neutrino sector with CMB data is to take account of the BBN-predicted helium-4 abundance as a prior rather than fixing the helium-4 abundance.

In this paper we investigate constraints on Lorentz invariance violation in the neutrino sector from a joint analysis of BBN and CMB. In combination with the latest measurement of the primordial helium-4 abundance, the Planck 2015 data of the CMB anisotropies give a strong constraint on the deformation parameter. Adding the primordial helium measurement can break effectively the degeneracy between the deformation parameter and the physical dark matter density.

This paper is organized as follows. In Sect. 2 we parameterize Lorentz invariance violation in the neutrino sector. In Sect. 3, we derive the weak reaction rates in the Lorentz-violating extension of the standard model and calculate the BBN prediction of the helium-4 abundance. In Sect. 4, we derive the Boltzmann equation for neutrinos in the synchronous gauge and calculate the CMB power spectrum. In Sect. 5, we place constraints on the deformation parameter using the Planck 2015 data in combination with the latest measurement of the primordial helium-4 abundance. Section 6 is devoted to our conclusions.

2 Deformed dispersion relation

At a phenomenological level, the deformed dispersion relation can be characterized by a power series of momentum. In this paper, we consider a simple instance of the dispersion relation for neutrinos constructed in [10], which can be parameterized as follows:

$$E^2 = m^2 + p^2 + \xi p^2, \tag{1}$$

where E is the neutrino energy, m the neutrino mass, $p = \left(p^i p_i\right)^{1/2}$ the magnitude of the 3-momentum, and ξ the

deformation parameter characterizing the Lorentz symmetry violation.

In the spatially flat Friedmann–Lemaintre–Robertson–Walker metric with the scale factor a, the number density n_ν, energy density ρ_ν and pressure P_ν for neutrinos with (1) are given by

$$n_\nu = \frac{1}{a^3} \int \frac{\mathrm{d}^3 q}{(2\pi)^3} f_0(q), \tag{2}$$

$$\rho_\nu = \frac{1}{a^4} \int \frac{\mathrm{d}^3 q}{(2\pi)^3} \epsilon f_0(q), \tag{3}$$

$$P_\nu = \frac{1}{3a^4} \int \frac{\mathrm{d}^3 q}{(2\pi)^3} \frac{(1+\xi) q^2}{\epsilon} f_0(q). \tag{4}$$

The phase space distribution for neutrinos is $f_0(q) = g_s \left[1 + \exp(\epsilon/T_0)\right]^{-1}$, where $g_s = 2$ is the number of spin degrees of freedom, T_0 the neutrino temperature today, q the magnitude of the comoving 3-momentum, and $\epsilon = \sqrt{m^2 a^2 + (1+\xi) q^2}$ the comoving energy.

3 BBN prediction

The abundances of the light elements produced during the BBN epoch depend on the competition between the nuclear and weak reaction rates and the expansion rate of the Universe. In the standard cosmological scenario and in the framework of the electroweak standard model, the dynamics of this phase is controlled by only one free parameter, the baryon to photon number density.

We consider N species of nuclides whose abundances X_i are the number densities n_i normalized with respect to the baryon number density n_B,

$$X_i = \frac{n_i}{n_B}, \quad i = n, p, {}^2H, \dots. \tag{5}$$

Their evolutions are ruled by the following Boltzmann equations:

$$\dot{X}_i = \sum_{j,k,l} N_i \left(\Gamma_{kl \to ij} \frac{X_l^{N_l} X_k^{N_k}}{N_l! \, N_k!} - \Gamma_{ij \to kl} \frac{X_i^{N_i} X_j^{N_j}}{N_i! \, N_j!} \right), \tag{6}$$

where Γ denotes the reaction rate and N_i is the number of nuclide i involved in the reaction.

In the case of Lorentz invariance violation in the neutrino sector, the changes of the reaction rates of the following weak reactions have to be taken into account:

$$n + \nu_e \leftrightarrow p + e^-, \tag{7}$$

$$n + e^+ \leftrightarrow p + \bar{\nu}_e, \tag{8}$$

$$n \leftrightarrow p + \bar{\nu}_e + e^-, \tag{9}$$

which determine the neutron-to-proton ratio when the baryons become uncoupled from the leptons. The abundances of the light elements depend on the neutron-to-proton ratio at the onset of BBN. As an example, let us compute the reaction rate of the process (7) in the Lorentz-violating extension of the standard model [20,24]. The reaction rate is [23]

$$\Gamma = \left[1 - \frac{3}{8}\xi - \frac{3\left(C_V^2 - C_A^2\right)}{4\left(C_V^2 + 3C_A^2\right)}\xi \right] (1+\xi)^{-3/2}\, \Gamma^{(0)}, \quad (10)$$

where C_V and C_A are the vector and axial coupling of the nucleon, $\Gamma^{(0)}$ is the standard reaction rate per incident nucleon derived in Ref. [25]. The first prefactor on the right-hand side of Eq. (10) arises from the neutrino propagator and the $e\nu W$ coupling in the Lorentz-violating extension of standard model. The second prefactor comes from the statistical distribution for neutrinos. As for the other processes in (7)–(9), their reaction rates can be simply derived by properly changing the statistical factors and the delta function determined by the energy conservation for each reaction. Therefore, the corrections to the conversion rate of neutron into proton and its inverse rate are the same as in (10).

In order to calculate the abundance of the light elements produced during the BBN epoch, we modified the publicly available PArthENoPE code [26] to appropriately incorporate the Lorentz-violating term in the neutrino sector. As shown in [23], the BBN-predicted abundance of helium-4 is sensitive to the deformed parameter ξ due to the fact that it is mainly determined by the neutron-to-proton ratio, which is related to the weak reaction rate, neutrino number density and expansion rate of the Universe. In our analysis we shall focus on the helium-4 abundance that influences the CMB power spectrum.

Although in our analysis we use an interpolation method to obtain the value of Y_p on a grid of points in $(\Omega_b h^2, \xi)$ space (see Sect. 5), it is possible to describe the dependencies of the BBN-predicted helium-4 abundances upon the two parameters by simple, linear fits which, over their ranges of applicability, are accurate to a few percent. Following [27], we get the following linear fit for Y_p versus $\Omega_b h^2$ and ξ:

$$Y_p^{\mathrm{FIT}} = 0.2334 + 0.52\Omega_b h^2 + 0.258\xi, \quad (11)$$

over our adopted range in $\Omega_b h^2$ and ξ, as shown in Fig. 1. We note that this fit is a very good approximation over the adopted parameter ranges, which is useful in facilitating studies of the viability of various options for non-standard physics and cosmology, prior to undertaking detailed BBN calculations

Since the neutrino species share the temperature with the photons prior to neutrino decoupling, the prediction for the effective number of neutrino species is

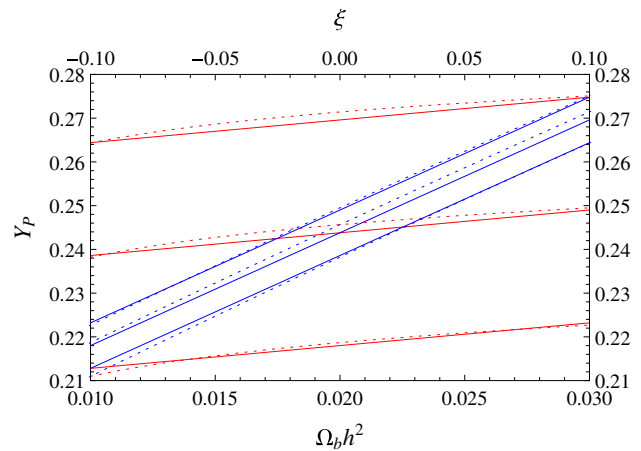$$N_{\mathrm{eff}} = 3.046(1+\xi)^{-3/2}. \quad (12)$$

Fig. 1 BBN-predicted curves for Y_p in $\Omega_b h^2$ (*red*) and ξ (*blue*). From *bottom* to *top*, the *red curves* correspond to $\xi = -0.1, 0, -0.1$, while the *blue curves* correspond to $\Omega_b h^2 = 0.01, 0.02, 0.03$. The *dotted curves* are the BBN-predicted results, while the *solid curves* are our fits

The total relativistic energy density ρ_r in neutrinos is given in terms of the photon density ρ_γ by

$$\rho_r = N_{\mathrm{eff}} \frac{7}{8} \left(\frac{4}{11}\right)^{4/3} \rho_\gamma. \quad (13)$$

4 CMB power spectrum

The Lorentz-violating term affects not only the evolution of the cosmological background but also the behavior of the neutrino perturbations. Following Ref. [28] we shall derive the Boltzmann equation of the distribution function for neutrinos with (1) to linear order in the perturbations. In the synchronous gauge, the perturbed energy density $\delta\rho_\nu$, pressure δP_ν, energy flux θ_ν, and shear stress σ_ν are, respectively, given by

$$\delta\rho_\nu = \frac{1}{a^4} \int \frac{\mathrm{d}^3 q}{(2\pi)^3} \epsilon f_0(q)\, \Psi_0, \quad (14)$$

$$\delta P_\nu = \frac{1}{3a^4} \int \frac{\mathrm{d}^3 q}{(2\pi)^3} \frac{(1+\xi)\, q^2}{\epsilon} f_0(q)\, \Psi_0, \quad (15)$$

$$(\rho_\nu + P_\nu)\theta_\nu = \frac{k}{a^4} \int \frac{\mathrm{d}^3 q}{(2\pi)^3} \sqrt{1+\xi}\, q f_0(q)\, \Psi_1, \quad (16)$$

$$(\rho_\nu + P_\nu)\sigma_\nu = \frac{2}{3a^4} \int \frac{\mathrm{d}^3 q}{(2\pi)^3} \frac{(1+\xi)\, q^2}{\epsilon} f_0(q)\, \Psi_2, \quad (17)$$

where Ψ_l are the expansion coefficients of the perturbed neutrino distribution function expanded in a series of Legendre polynomials

$$\Psi(\vec{k}, \hat{n}, q, \tau) = \sum_{\ell=0}^{\infty} (-i)^\ell (2\ell+1) \Psi_\ell(\vec{k}, q, \tau) P_\ell(\hat{k}\cdot\hat{n}), \quad (18)$$

where τ is the conformal time. These perturbations Ψ_l satisfy the following Boltzmann equations:

$$\dot{\Psi}_\ell + (1+\xi)\frac{q}{\epsilon}\frac{k}{2\ell+1}\left[(\ell+1)\Psi_{\ell+1} - \ell\Psi_{\ell-1}\right]$$
$$+ \left(\delta_{2\ell}\frac{1}{15}\dot{h} + \delta_{2\ell}\frac{2}{5}\dot{\eta} - \delta_{0\ell}\frac{1}{6}\dot{h}\right)\frac{\mathrm{d}\ln f_0}{\mathrm{d}\ln q} = 0, \qquad (19)$$

in the synchronous gauge, where dots denote derivatives with respect to the conformal time, h and η are the two scalar modes of the metric perturbations in the Fourier space k. To avoid the reflections from high-ℓ equations by simply set $\Psi_\ell = 0$ for $\ell > \ell_{\max}$, such a Boltzmann hierarchy is effectively truncated by adopting the following scheme [28]:

$$\Psi_{\ell_{\max}+1} \approx \frac{(2\ell_{\max}+1)\epsilon}{(1+\xi)\,qk\tau}\Psi_{\ell_{\max}} - \Psi_{\ell_{\max}-1}. \qquad (20)$$

Making a transformation $q \to \sqrt{1+\xi}q$, we note that the number density, energy density and pressure of neutrinos are proportional to $(1+\xi)^{-3/2}$, which means that increasing ξ decreases the number density, energy density and pressure of neutrinos. Moreover, there is a factor $\sqrt{1+\xi}$ in the second term of the Boltzmann equations, which comes from neutrino propagation.

For the massless neutrinos, the Boltzmann equations are simplified by setting $\epsilon = \sqrt{1+\xi}q$. The number of variables can be reduced by integrating out the q dependence in the neutrino distribution function so that

$$F(\vec{k}, \hat{n}, \tau) = \frac{\int q^2 dq\epsilon f_0(q)\Psi}{\int q^2 dq\epsilon f_0(q)}$$
$$= \sum_{\ell=0}^{\infty}(-i)^\ell(2\ell+1)F_\ell(\vec{k}, \tau)P_\ell(\hat{k}\cdot\hat{n}). \qquad (21)$$

Using the orthonormality and recursion relation of the Legendre polynomials, from the Boltzmann equations we derive the evolution equations of the perturbed energy density $\delta_\nu = \delta\rho_\nu/\rho_\nu$, energy flux θ_ν, shear stress σ_ν independent of the momentum q,

$$\dot{\delta}_\nu = -\frac{4}{3}\sqrt{1+\xi}\theta_\nu - \frac{2}{3}\dot{h}, \qquad (22)$$

$$\dot{\theta}_\nu = \sqrt{1+\xi}k^2\left(\frac{1}{4}\delta_\nu - \sigma_\nu\right), \qquad (23)$$

$$2\dot{\sigma}_\nu = \sqrt{1+\xi}\frac{8}{15}\theta_\nu - \frac{3}{5}\sqrt{1+\xi}kF_3 + \frac{4}{15}\dot{h} + \frac{8}{5}\dot{\eta}, \qquad (24)$$

$$\dot{F}_\ell = \frac{\sqrt{1+\xi}k}{2\ell+1}\left[\ell F_{\ell-1} - (\ell+1)F_{\ell+1}\right], \quad \ell \geq 3. \qquad (25)$$

The truncation scheme for massless neutrinos is

$$F_{\ell_{\max}+1} \approx \frac{(2\ell_{\max}+1)}{\sqrt{1+\xi}k\tau}F_{\ell_{\max}} - F_{\ell_{\max}-1}. \qquad (26)$$

In the synchronous gauge the adiabatic initial conditions for the metric perturbations and massless neutrinos in the cold dark matter frame are

$$h = Ck^2\tau^2 - \frac{1}{5}C\omega k^2\tau^3, \qquad (27)$$

$$\eta = 2C - \frac{5 - 5R_\nu + 9R_\nu\sqrt{1+\xi}}{6\left(15 + 4R_\nu\sqrt{1+\xi}\right)}Ck^2\tau^2, \qquad (28)$$

$$\delta_\nu = -\frac{2}{3}Ck^2\tau^2 + \frac{2}{15}C\omega k^2\tau^3, \qquad (29)$$

$$\theta_\nu = -\frac{(23 + 4R_\nu)\sqrt{1+\xi}}{18\left(15 + 4R_\nu\sqrt{1+\xi}\right)}Ck^4\tau^3, \qquad (30)$$

$$\sigma_\nu = \frac{2\left(2 + R_\nu - R_\nu\sqrt{1+\xi}\right)}{3\left(15 + 4R_\nu\sqrt{1+\xi}\right)}Ck^2\tau^2$$
$$- \frac{25 + R_\nu\left(65 - 85\sqrt{1+\xi}\right) + 4R_\nu^2\left(\sqrt{1+\xi} - 1 - \xi\right)}{15\left(15 + 2R_\nu\sqrt{1+\xi}\right)\left(15 + 4R_\nu\sqrt{1+\xi}\right)}$$
$$\times C\omega k^2\tau^3, \qquad (31)$$

$$F_3 = \frac{4}{21}\frac{2\sqrt{1+\xi} + R_\nu\left(\sqrt{1+\xi} - 1 - \xi\right)}{15 + 4R_\nu\sqrt{1+\xi}}Ck^3\tau^3, \qquad (32)$$

where C is a dimensionless constant determined by the amplitude of the fluctuations from inflation, $R_\nu \equiv \rho_\nu/(\rho_\gamma + \rho_\nu)$, and $\omega \equiv \Omega_m H_0/\sqrt{\Omega_\gamma + \Omega_\nu}$, which corresponds to the matter contribution to the total energy density of the Universe. In the radiation-dominated era the massive neutrinos are relativistic. The initial condition of Ψ_0 for massive neutrinos is related to δ_ν. Then, using Eqs. (19) and ignoring the mass terms in the differential equations of high-order moment, we get the initial conditions of Ψ_ℓ for massive neutrinos:

$$\Psi_0 = -\frac{1}{4}\delta_\nu\frac{\mathrm{d}\ln f_0}{\mathrm{d}\ln q}, \qquad (33)$$

$$\Psi_1 = -\frac{\epsilon}{3\sqrt{1+\xi}qk}\theta_\nu\frac{\mathrm{d}\ln f_0}{\mathrm{d}\ln q}, \qquad (34)$$

$$\Psi_2 = -\frac{1}{2(1+\xi)}\left(\sigma_\nu + \frac{1}{4}\xi\delta_\nu\right)\frac{\mathrm{d}\ln f_0}{\mathrm{d}\ln q}, \qquad (35)$$

$$\Psi_\ell = 0, \quad \ell \geq 3. \qquad (36)$$

In order to compute the theoretical CMB power spectrum, we modified the Boltzmann CAMB code [29] to appropriately incorporate the Lorentz-violating term in the neutrino sector. As pointed out in [22], the effects of the Lorentz-violating term on the CMB power spectrum are distinguished from a change in the total mass of neutrinos or in the effective number of extra relativistic species [30–34]. Therefore, the measurements of the CMB anisotropies provide a cosmological probe of Lorentz invariance violation in the neutrino sector. Moreover, we calculate the matter power spectrum today for $\xi = -0.1, 0, 0.1$. From Fig. 2 we find that increasing ξ can enhance the matter power spectrum at small scales. It is well known that variances in the helium-4 abundance modify the density of free electrons between helium and hydrogen recombination and therefore influence the CMB power spec-
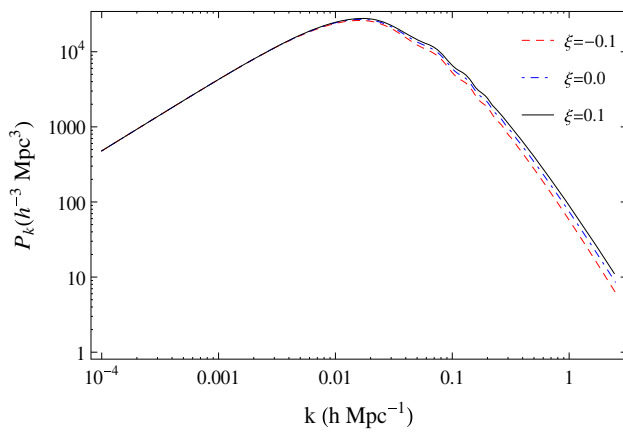
Fig. 2 The matter power spectrum for $\xi = -0.1$ (*dashed*), 0 (*dash-dotted*), 0.1 (*solid*)

trum. However, the effects of the Lorentz-violating term on the BBN-predicted helium-4 abundance were not considered in [22]. In the next section, we shall put constraints on the deformation parameter from a joint analysis of BBN and CMB.

5 Joint analysis from BBN and CMB

In our analysis we use a modified version of the publicly available CosmoMC package to explore the parameter space by means of Monte Carlo Markov chains technique [35]. Since the deformation parameter ξ is nearly uncorrelated with the total mass of neutrinos when CMB data are used to detect the signature of Lorentz invariance violence [22], we only consider massless neutrinos with vanishing chem-

ical potentials in our analysis. Our cosmological model is the spatially flat ΛCDM plus three types of massless neutrino with the deformed dispersion relation (1), which can be described by the following seven parameters:

$$\{\Omega_b h^2, \Omega_c h^2, \theta_{MC}, \tau_{re}, n_s, A_s, \xi\},$$

where h is the dimensionless Hubble parameter defined by $H_0 = 100h \, \text{km s}^{-1} \, \text{Mpc}^{-1}$, $\Omega_b h^2$ and $\Omega_c h^2$ are the physical baryon and dark matter densities relative to the critical density, θ_{MC} is an approximation to the ratio of the sound horizon to the angular diameter distance at the photon decoupling, τ_{re} is the reionization optical depth, n_s and A_s are the spectral index and amplitude of the primordial curvature perturbations at the pivot scale $k_0 = 0.05 \, \text{Mpc}^{-1}$.

We firstly run the PArthENoPE BBN code with two free input parameters, $\Omega_b h^2$ and ξ, to precalculate the primordial helium-4 abundance on a grid of points in ($\Omega_b h^2$, ξ) space. For each couple of parameter values the helium-4 abundances are then obtained from the grid by two-dimensional cubic spline interpolation, which is adopted to calculate the CMB power spectrum. This method is called "BBN consistency".

We use the recently released Planck 2015 likelihood code and data, including the Planck low-ℓ likelihood at multipoles $2 \leq \ell \leq 29$ and Planck high-ℓ likelihood at multipoles $\ell \geq 30$ based on pseudo-C_ℓ estimators [5]. The former uses foreground-cleaned LFI 70 GHz polarization maps together with the temperature map obtained from the Planck 30 to 353 GHz channels by the Commander component separation algorithm over 94% of the sky. The latter uses 100, 143, and 217 GHz half-mission cross-power spectra, avoiding the galactic plane as well as the brightest point sources and the regions where the CO emission is the strongest. "Planck

Table 1 Mean values and marginalized 68% confidence level for the deformation parameter and other cosmological parameters, derived from the Planck data in combination with baryon acoustic oscillation data, the JLA sample of Type Ia supernovae and the measurement of the helium-4 mass fraction. For comparison with BBN consistency, fixing $Y_p = 0.24$ is also considered
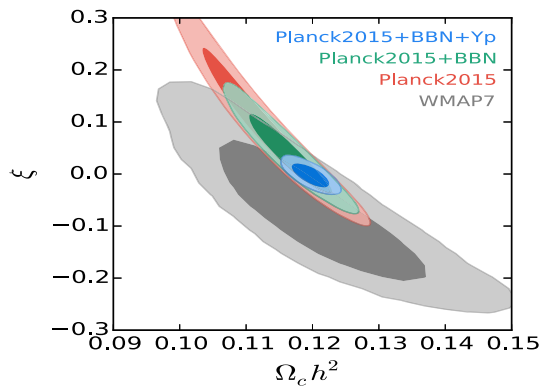
Model	Planck 2015 + JLA + BAO		Planck 2015 + JLA + BAO + Y_p
	$Y_p = 0.24$ (fixed)	BBN consistency	BBN consistency
$\Omega_b h^2$	0.02127 ± 0.00046	0.02212 ± 0.00025	0.02227 ± 0.00021
$\Omega_c h^2$	0.1124 ± 0.0061	0.1163 ± 0.0040	0.1197 ± 0.0018
$100\theta_{MC}$	1.04181 ± 0.00098	1.04173 ± 0.00101	1.04090 ± 0.00050
τ_{re}	0.071 ± 0.018	0.076 ± 0.018	0.077 ± 0.018
n_s	0.9583 ± 0.0069	0.9679 ± 0.0049	0.9659 ± 0.0044
$\ln(10^{10} A_s)$	3.064 ± 0.038	3.084 ± 0.035	3.087 ± 0.035
H_0 (km s^{-1} Mpc^{-1})	65.92 ± 1.76	67.25 ± 1.00	68.01 ± 0.63
σ_8	0.840 ± 0.014	0.846 ± 0.016	0.841 ± 0.015
Age (Gyr)	14.191 ± 0.35	13.937 ± 0.19	13.767 ± 0.068
Ω_Λ	0.691 ± 0.008	0.694 ± 0.007	0.693 ± 0.007
Ω_m	0.309 ± 0.008	0.306 ± 0.007	0.307 ± 0.007
ξ	0.101 ± 0.091	0.042 ± 0.049	-0.002 ± 0.014

Fig. 3 Marginalized two-dimensional contours in the $\xi - \Omega_c h^2$ plane with 68 and 95% confidence level in the extended ΛCDM model with BBN consistency, derived from the data of Planck 2015 + JLA + BAO (*green*) and Planck 2015 + JLA + BAO + Y_p (*blue*). The *red* and *gray* contours correspond to $Y_p = 0.24$, derived from Planck 2015 + JLA + BAO and from WMAP7 + H_0 + BAO [22], respectively

2015" denotes the combination of the low-ℓ temperature-polarization likelihood and the high-ℓ temperature likelihood.

We use the "Joint Light-curve Analysis" (JLA) sample of type Ia supernovae, which is constructed from the SNLS and SDSS supernova data, together with several samples of low-redshift supernovae [36]. Baryon acoustic oscillation (BAO) measurements are another important astrophysical data set, which are powerful to break parameter degeneracies from CMB measurements. We use BAO measurements of $D_V/r_{\rm drag}$ from the 6dFGS at $z_{\rm eff} = 0.106$, SDSS Main Galaxy Sample at $z_{\rm eff} = 0.15$, BOSS LOWZ at $z_{\rm eff} = 0.32$, and BOSS CMASS at $z_{\rm eff} = 0.57$ [5]. Here D_V is the effective distance measure for angular diameter distance, $r_{\rm drag}$ is the comoving sound horizon at the end of the baryon drag epoch and $z_{\rm eff}$ is the effective redshift. In our analysis we also use the helium-4 mass fraction measurement of $Y_p = 0.2449 \pm 0.0040$, derived from helium and hydrogen emission lines from metal-poor extragalactic HII regions and from a regression to zero metallicity [37].

In Table 1 we list our results. With the combined data of Planck 2015+JLA+BAO, the deformation parameter is estimated to be $\xi = 0.042 \pm 0.049$ if the helium-4 abundance is set from the BBN prediction. For comparison, if the helium-4

Fig. 4 Marginalized two-dimensional contours in $\xi - \Omega_b h^2$ (*top-left*), $\xi - H_0$ (*top-right*), $\xi - n_s$ (*bottom-left*) and $\xi - A_s$ (*bottom-right*), with 68 and 95% confidence level in the extended ΛCDM model with BBN consistency, derived from the data of Planck 2015 + JLA + BAO (*green*) and Planck 2015 + JLA + BAO + Y_p (*blue*). The *red contours* correspond to $Y_p = 0.24$, derived from Planck 2015 + JLA + BAO

abundance is not varied independently of other parameters, with the same data set we find $\xi = 0.101 \pm 0.091$, which indicates that the constraint of ξ is not improved compared to the result derived in [22] from the 7-year WMAP [38] in combination with lower-redshift measurements of the expansion rate. The reason is that the estimated values of cosmological parameters are biased by fixing $Y_p = 0.24$. The gray and red regions in Fig. 3 show 68 and 95% contours in the $\xi - \Omega_c h^2$ plane setting $Y_p = 0.24$, derived from Planck 2015+JLA+BAO and from WMAP7 + H_0 + BAO [22], respectively. We see that the Planck 2015 data marginally favor a positive ξ compared to the 7-year WMAP data. The addition of the latest measurement of the helium-4 abundance leads to a strong constraint on the deformation parameter $\xi = -0.002 \pm 0.014$. As shown in Fig. 3, adding the Y_p data breaks the degeneracy between the deformation parameter and the physical dark matter density. This result shows that no signal of Lorentz invariant violation is detected by the joint analysis of CMB and BBN. Figure 4 shows the constraints in the $\xi - \Omega_b h^2$ plane, $\xi - H_0$ plane, $\xi - n_s$ plane and $\xi - A_s$ plane from Planck 2015 + JLA + BAO.

6 Conclusions and discussions

We have studied the cosmological constraints on Lorentz invariance violation in the neutrino sector by a joint analysis of CMB and BBN. Instead of fixing the value of the helium-4 abundance, we have applied the BBN prediction of the helium-4 abundance determined by ξ and $\Omega_b h^2$ to calculate the CMB power spectra. Using the Planck 2015 data in combination with the JLA sample of type Ia supernovae and the BAO feature, we have put a constraint on the deformation parameter. Adding the measurement of the helium-4 abundance breaks the degeneracy between the deformation parameter and the physical dark matter density and so improves the constraint by a factor 3.

As found in [22], the deformation parameter is nearly uncorrelated with the total mass of neutrinos Σm_ν when WMAP data are used to constrain ξ. Planck 2015 data is much more sensitive to the total mass of neutrinos than WMAP data. Therefore, we consider the effects of the neutrino masses on our results. Figure 5 shows 68 and 95% contours in the $\xi - \Sigma m_\nu$ plane for Planck 2015 data combined with lower-redshift measurements. We see that ξ is nearly uncorrelated with Σm_ν from Fig. 5.

Compared to cosmological bounds on the Lorentz-violating coefficient, observations of high-energy astrophysical neutrinos give stronger constraints. As listed in Table XIII of Ref. [13], the coefficient is constrained down to $\mathcal{O}(10^{-9})$ from the time-of-flight measurements, under the assumption that neutrino oscillations are negligible. Cohen and Glashow have argued that the observation of neutrinos with energies
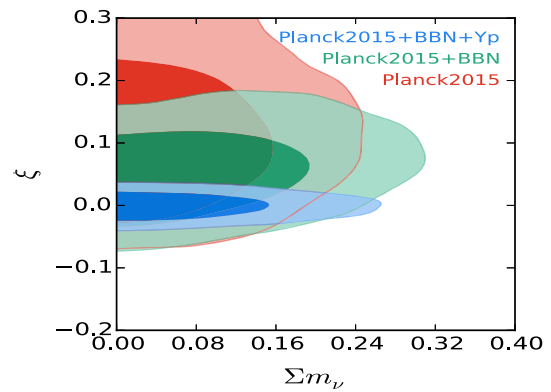

Fig. 5 Marginalized two-dimensional contours in the $\xi - \Sigma m_\nu$ plane with 68 and 95% confidence level in the extended ΛCDM model with BBN consistency, derived from the data of Planck 2015 + JLA + BAO (*green*) and Planck 2015 + JLA + BAO + Y_p (*blue*). The *red contours* correspond to $Y_p = 0.24$, derived from Planck 2015 + JLA + BAO

in excess of 100 TeV and a baseline of at least 500 km allows us to deduce that the Lorentz-violating parameter is less than $\mathcal{O}(10^{-11})$ [39]. The present work provides a new way to probe the signal of Lorentz invariance violation in the early Universe, which can in principle be used to constrain ξ in the sterile neutrino sector [40,41]. Although present cosmological data are too weak to yield competitive constraints, future measurements of CMB and BBN offer prospects for placing stringent constraints.

References

1. M.C. Gonzalez-Garcia, M. Maltoni, Phys. Rept. **460**, 1 (2008). arXiv:0704.1800 [hep-ph]
2. M. Kaplinghat, L. Knox, Y.S. Song, Phys. Rev. Lett. **91**, 241301 (2003). arXiv:astro-ph/0303344
3. J. Lesgourgues, L. Perotto, S. Pastor, M. Piat, Phys. Rev. D **73**, 045021 (2006). arXiv:astro-ph/0511735
4. J. Lesgourgues, S. Pastor, Adv. High Energy Phys. **2012**, 608515 (2012). arXiv:1212.6154 [hep-ph]
5. P.A.R. Ade et al. [Planck Collaboration], Astron. Astrophys. **594**, A13 (2016). arXiv:1502.01589 [astro-ph.CO]

6. W. Hu, D.J. Eisenstein, M. Tegmark, Phys. Rev. Lett. **80**, 5255 (1998). arXiv:astro-ph/9712057
7. A. Ringwald, Y.Y.Y. Wong, JCAP **0412**, 005 (2004). arXiv:hep-ph/0408241
8. Y.Y.Y. Wong, Ann. Rev. Nucl. Part. Sci. **61**, 69 (2011). arXiv:1111.1436 [astro-ph.CO]
9. S.R. Coleman, S.L. Glashow, Phys. Lett. B **405**, 249 (1997). arXiv:hep-ph/9703240
10. S.R. Coleman, S.L. Glashow, Phys. Rev. D **59**, 116008 (1999). arXiv:hep-ph/9812418
11. V.A. Kostelecky, M. Mewes, Phys. Rev. D **70**, 031902 (2004). arXiv:hep-ph/0308300
12. V.A. Kostelecky, M. Mewes, Phys. Rev. D **69**, 016005 (2004). arXiv:hep-ph/0309025
13. A. Kostelecky, M. Mewes, Phys. Rev. D **85**, 096005 (2012). arXiv:1112.6395 [hep-ph]
14. I. Motie, S.S. Xue, Int. J. Mod. Phys. A **27**, 1250104 (2012). arXiv:1206.0709 [hep-ph]
15. J.S. Diaz, A. Kostelecky, M. Mewes, Phys. Rev. D **89**(4), 043005 (2014). arXiv:1308.6344 [astro-ph.HE]
16. G. Amelino-Camelia, New J. Phys. **6**, 188 (2004). arXiv:gr-qc/0212002
17. J. Alfaro, H.A. Morales-Tecotl, L.F. Urrutia, Phys. Rev. Lett. **84**, 2318 (2000). arXiv:gr-qc/9909079
18. S.M. Carroll, J.A. Harvey, V.A. Kostelecky, C.D. Lane, T. Okamoto, Phys. Rev. Lett. **87**, 141601 (2001). arXiv:hep-th/0105082
19. J. Magueijo, L. Smolin, Phys. Rev. Lett. **88**, 190403 (2002). arXiv:hep-th/0112090
20. D. Colladay, V.A. Kostelecky, Phys. Rev. D **58**, 116002 (1998). arXiv:hep-ph/9809521
21. V.A. Kostelecky, N. Russell, Rev. Mod. Phys. **83**, 11 (2011). arXiv:0801.0287 [hep-ph]
22. Z.K. Guo, Q.G. Huang, R.G. Cai, Y.Z. Zhang, Phys. Rev. D **86**, 065004 (2012). arXiv:1206.5588 [astro-ph.CO]
23. Z.K. Guo, J.W. Hu, Phys. Rev. D **87**(12), 123519 (2013). arXiv:1303.2813 [astro-ph.CO]
24. G. Lambiase, Phys. Rev. D **72**, 087702 (2005). arXiv:astro-ph/0510386
25. R.E. Lopez, M.S. Turner, Phys. Rev. D **59**, 103502 (1999). arXiv:astro-ph/9807279
26. O. Pisanti, A. Cirillo, S. Esposito, F. Iocco, G. Mangano, G. Miele, P.D. Serpico, Comput. Phys. Commun. **178**, 956 (2008). arXiv:0705.0290 [astro-ph]
27. J.P. Kneller, G. Steigman, New J. Phys. **6**, 117 (2004). arXiv:astro-ph/0406320
28. C.P. Ma, E. Bertschinger, Astrophys. J. **455**, 7 (1995). arXiv:astro-ph/9506072
29. A. Lewis, A. Challinor, A. Lasenby, Astrophys. J. **538**, 473 (2000). arXiv:astro-ph/9911177
30. W. Hu, D. Scott, N. Sugiyama, M.J. White, Phys. Rev. D **52**, 5498 (1995). arXiv:astro-ph/9505043
31. S. Bashinsky, U. Seljak, Phys. Rev. D **69**, 083002 (2004). arXiv:astro-ph/0310198
32. J. Hamann, S. Hannestad, G.G. Raffelt, Y.Y.Y. Wong, JCAP **0708**, 021 (2007). arXiv:0705.0440 [astro-ph]
33. Z. Hou, R. Keisler, L. Knox, M. Millea, C. Reichardt, Phys. Rev. D **87**, 083008 (2013). arXiv:1104.2333 [astro-ph.CO]
34. Z.K. Guo, Y.Z. Zhang, Phys. Rev. D **85**, 103519 (2012). arXiv:1201.1538 [astro-ph.CO]
35. A. Lewis, S. Bridle, Phys. Rev. D **66**, 103511 (2002). arXiv:astro-ph/0205436
36. M. Betoule et al, [SDSS Collaboration], Astron. Astrophys. **552**, A124 (2013). arXiv:1212.4864 [astro-ph.CO]
37. E. Aver, K.A. Olive, E.D. Skillman, JCAP **1507**(07), 011 (2015). arXiv:1503.08146 [astro-ph.CO]
38. E. Komatsu et al, [WMAP Collaboration], Astrophys. J. Suppl. **192**, 18 (2011). arXiv:1001.4538 [astro-ph.CO]
39. A.G. Cohen, S.L. Glashow, Phys. Rev. Lett. **107**, 181803 (2011). arXiv:1109.6562 [hep-ph]
40. J. Hamann, S. Hannestad, G.G. Raffelt, I. Tamborra, Y.Y.Y. Wong, Phys. Rev. Lett. **105**, 181301 (2010). arXiv:1006.5276 [hep-ph]
41. J. Hamann, S. Hannestad, G.G. Raffelt, Y.Y.Y. Wong, JCAP **1109**, 034 (2011). arXiv:1108.4136 [astro-ph.CO]